

# TTN-AS1 accelerates the growth and migration of nasopharyngeal carcinoma cells via targeting miR-876-5p/NETO2

Xinping Chen,<sup>1,2</sup> Weihua Xu,<sup>1,2</sup> Zhichao Ma,<sup>1</sup> Juan Zhu,<sup>1</sup> Junjie Hu,<sup>1</sup> Xiaojuan Li,<sup>1</sup> and Shengmiao Fu<sup>1</sup>

<sup>1</sup>Central Laboratory, Hainan General Hospital, Hainan Hospital Affiliated to the Hainan Medical College, No. 19 Xiuhua Road, Xiuying District, Haikou, Hainan, 570311, China

**Nasopharyngeal carcinoma (NPC) is one of the most predominant cancers occurring in China with high morbidity. Lately, large quantities of long non-coding RNAs (lncRNAs) have been highlighted to regulate the biological activities in multiple tumors, including NPC. Our study centered on whether TTN-AS1 was involved in NPC and how it modulated the progression of NPC. Here, qRT-PCR data uncovered that TTN-AS1 expression was conspicuously high in NPC cells. Based on the results of functional assays, TTN-AS1 silence hampered the proliferative, migratory, and invasive abilities but stimulated the apoptotic capability of NPC cells. After a series of mechanism assays, TTN-AS1 was found to competitively bind with miR-876-5p and recruit UPF1 to enhance NETO2 expression. In addition, TTN-AS1 could be transcriptionally activated by YY1 in NPC cells. It was also found that miR-876-5p overexpression or NETO2 downregulation had inhibitory effects on cell proliferation, migration, and invasion in NPC. Moreover, NETO2 upregulation could restore the suppressive impacts of TTN-AS1 depletion on NPC cell and tumor growth. In conclusion, YY1-activated TTN-AS1 interacted with both miR-876-5p and UPF1 to upregulate NETO2, thus strengthening NPC cell malignant behaviors, which might provide more useful information for people to develop effective NPC treatments.**

## INTRODUCTION

Nasopharyngeal carcinoma (NPC) is a typical cancer with distinct geographical features. It is widespread in south China and Southeast Asia.<sup>1</sup> Multiple factors can lead to NPC occurrence, such as hereditary factors, environmental factors, and Epstein-Barr virus infection, among which the environmental factors are rather crucial.<sup>2,3</sup> With the appliance of radiotherapy and chemotherapy as well as the combined therapy, the results of treatment have a great improvement.<sup>4,5</sup> Meanwhile, the distant metastasis has become the primary barrier in treating NPC patients at middle and advanced stages.<sup>6</sup> Hence, it is necessary to have a deep comprehension of NPC mechanism for developing probable biomarkers or targets for NPC.

With the development of molecular biology, a host of non-coding RNAs (ncRNAs), which have limited protein-coding capabilities,

have been identified and illustrated to have crucial functions in the progression of cancers. Long non-coding RNAs (lncRNAs) are a class of ncRNAs of no less than 200 nt in length,<sup>7</sup> and their importance has already been reported in cancers, including NPC. For example, DANCR accelerates NPC metastasis by stabilizing HIF-1 $\alpha$  and interacting with NF90/NF45.<sup>8</sup> HOTAIR prompts cell invasion and migration in NPC through targeting miR-101/COX-2.<sup>9</sup> AFAP1-AS1 promotes the progression of NPC via modulation of the Rho/Rac pathway.<sup>10</sup> Nonetheless, most lncRNAs have not been studied in NPC. TTN-AS1 has been reported to have oncogenic functions in cervical cancer by targeting miR-573/E2F3.<sup>11</sup> TTN-AS1 influences osteosarcoma cell apoptosis and drug resistance through the modulation of the miR-134-5p/MBTD1 axis.<sup>12</sup> TTN-AS1 competitively binds with miR-376a-3p to push colorectal cancer progression via upregulating KLF15.<sup>13</sup> The TTN-AS1/miR133b/FSCN1 regulatory axis has been uncovered to be a bona fide target for anti-esophageal squamous cell carcinoma therapies.<sup>14</sup> However, there is still insufficient research focusing on the link between TTN-AS1 and NPC.

lncRNAs have been identified to function as the sponges of microRNAs (miRNAs) so that the bound mRNAs are released to exert their functions. This mechanism is defined as the competing endogenous RNA (ceRNA) network.<sup>15</sup> For example, LINC00641 suppresses bladder cancer cell growth via targeting the miR-197-3p/KLF10/PTENPI3K/AKT pathway.<sup>16</sup> RMRP boosts the progression of gastric cancer via acting as the sponge of miR-206.<sup>17</sup> In our study, we analyzed whether TTN-AS1 functioned in NPC via a ceRNA network.

RNA-protein interaction plays a vital role in modulating biological processes,<sup>18</sup> especially the interplay between RNAs and RNA binding

Received 21 March 2021; accepted 18 November 2021;  
<https://doi.org/10.1016/j.omto.2021.11.009>.

<sup>2</sup>The author have contributed equally to this work

**Correspondence:** Shengmiao Fu, Central Laboratory, Hainan General Hospital, Hainan Hospital Affiliated to the Hainan Medical College, No. 19 Xiuhua Road, Xiuying District, Haikou, Hainan, 570311, China.

E-mail: [fusm58@126.com](mailto:fusm58@126.com)



proteins (RBPs). For example, OTUB2 stabilizes U2AF2 to benefit the development of non-small cell lung cancer.<sup>19</sup> In this study, we also wondered whether certain RBP was implicated in TTN-AS1-regulated NPC development.

The primary target of our study was to figure out the role of TTN-AS1 in NPC cells and make clear how TTN-AS1 affected NPC cell functions, which might provide novel promising targets to treat patients with NPC.

## RESULTS

### **TTN-AS1 is upregulated in NPC cells compared with NP69 cells and expedites the growth, migration, and invasion of NPC cells**

To thoroughly understand the impact of TTN-AS1 in NPC cells, we first measured the expression of TTN-AS1. Data of quantitative reverse-transcription polymerase chain reaction (qRT-PCR) attested that the expression of TTN-AS1 was aberrantly high in NPC cell lines (13-9B, 5-8F, C17, and C666-1) in comparison with normal NP69 cells, particularly in C17 and C666-1 cells (Figure 1A). Thus, we chose C17 and C666-1 cells for the following research. Next, we delved into the function of TTN-AS1 in NPC cells through testing the changes on cell behaviors when silencing TTN-AS1. As proved by qRT-PCR, TTN-AS1 expression was conspicuously suppressed by transfecting short hairpin (sh)/TTN-AS1#1/2 into C17 and C666-1 cells (Figure 1B). The results of colony formation and cell counting kit-8 (CCK-8) assays then revealed that the proliferative capacities of NPC cells were inhibited in response to the downregulation of TTN-AS1 (Figures 1C and 1D). Likewise, the migratory and invasive abilities were also weakened when TTN-AS1 was downregulated in NPC cells (Figures 1E and 1F). On the contrary, the apoptosis rate of these two cells was increased due to TTN-AS1 knockdown, based on the outcomes of flow cytometry analysis and a terminal deoxynucleotidyl transferase-mediated dUTP nick end labeling (TUNEL) assay (Figures 1G and 1H). In brief, TTN-AS1 is upregulated in NPC cells compared with NP69 cells and it promotes the oncogenic process of NPC cells.

### **MiR-876-5p represses the malignant behaviors of NPC cells**

To find out the cellular mechanism of TTN-AS1 in NPC cells, we then detected the localization of TTN-AS1 in NPC cells. The outcome of a fluorescence *in situ* hybridization (FISH) assay unveiled that TTN-AS1 was primarily accumulated in the cytoplasm rather than in the nucleus of both C17 and C666-1 cells (Figure 2A), which indicated the possibility for TTN-AS1 to participate in post-transcriptional regulation. Then, through jointly analyzing DIANA ([http://carolina.imis.athena-innovation.gr/diana\\_tools/web/index.php](http://carolina.imis.athena-innovation.gr/diana_tools/web/index.php)) and starBase (<http://starbase.sysu.edu.cn>), we discovered five common miRNAs that could bind with TTN-AS1 (Figure 2B). The expression of the five miRNAs was detected in NPC cells and NP69 cells. The results manifested that only miR-876-5p was obviously poorly expressed in NPC cells compared with normal cells (Figure 2C). According to bioinformatics prediction, we found an alignment between miR-876-5p and TTN-AS1 (Figure 2D). As revealed by RNA pull-down assays, TTN-AS1 was substantially

precipitated by biotinylated wild-type miR-876-5p (Bio-miR-876-5p-Wt) (Figure 2E), which suggested that miR-876-5p bound with TTN-AS1 at the indicated sites. Afterward, we overexpressed miR-876-5p via transfecting miR-876-5p mimics into NPC cells (Figure 2F). Luciferase reporter assays showed that miR-876-5p augmentation reduced the luciferase activity of TTN-AS1-Wt, while it had little impact on that of mutant TTN-AS1 (TTN-AS1-Mut) (Figure 2G), which reconfirmed the binding between TTN-AS1 and miR-876-5p on the putative sites. Next, we studied the influences of miR-876-5p on NPC cells. It was indicated that the proliferative capability of C17 and C666-1 cells was inhibited by miR-876-5p upregulation (Figures 2H and 2I). Similarly, elevation of miR-876-5p suppressed the migratory and invasive abilities of NPC cells (Figures 2J and 2K). Conversely, the NPC cell apoptosis rate was elevated owing to overexpression of miR-876-5p (Figures 2L and 2M). To conclude, the tumor-repressive miR-876-5p is sponged by TTN-AS1 in NPC cells.

### **NETO2 targeted by miR-876-5p promotes the proliferative, migratory, and invasive capabilities of NPC cells but restrains cell apoptosis**

StarBase predicted that there were five mRNAs possessing binding sites on miR-876-5p (CLIP data  $\geq 5$ , Degradome data  $\geq 3$  or 4 cancer types). Next, after transfecting miR-876-5p mimics, we found that only the expression of NETO2 was diminished prominently while no changes in that of other mRNAs were observed (Figure 3A). We also performed qRT-PCR and western blot assays to detect expression of NETO2 in NP69 and NPC cells. As shown in Figure S1A, NETO2 was expressed at a higher level in NPC cells, in contrast to NP69 cells. Bioinformatics tools were employed to project the underlying binding sites between miR-876-5p and NETO2 (Figure 3B). Then, RNA pull-down results illustrated that miR-876-5p bound with NETO2 in C666-1 and C17 cells at the predicted sites (Figure 3C). Afterward, luciferase reporter assays reconfirmed the binding of miR-876-5p to NETO2 at the indicated sites (Figure 3D). Later, the outcomes of RNA binding protein immunoprecipitation (RIP) assays showed that TTN-AS1, miR-876-5p, and NETO2 were all enriched in Argonaute 2 (Ago2) antibody but not in immunoglobulin G (IgG) antibody (Figure 3E), which signified the interactive relationship of miR-876-5p with TTN-AS1 and NETO2 in RNA-induced silencing complexes (RISCs). As seen from Figure 3F, TTN-AS1 was overexpressed in C666-1 and C17 cells by transfection of pcDNA3.1/TTN-AS1. In response to TTN-AS1 augmentation, the enrichment of NETO2 was lessened in the RISC complex, indicating that the binding of NETO2 and miR-876-5p declined in NPC cells (Figure S1B). Subsequently, the collected data from qRT-PCR and western blots showed that NETO2 expression was reduced by upregulation of miR-876-5p and then recovered by overexpression of TTN-AS1 (Figures 3G and S1C). Afterward, we explored the effects of NETO2 on NPC cells. Prior to that, we performed qRT-PCR and Western blot assays, finding that the expression of NETO2 in NPC cells was lowered by transfecting sh/NETO2#1/2 (Figures 3H and S1D). Next,

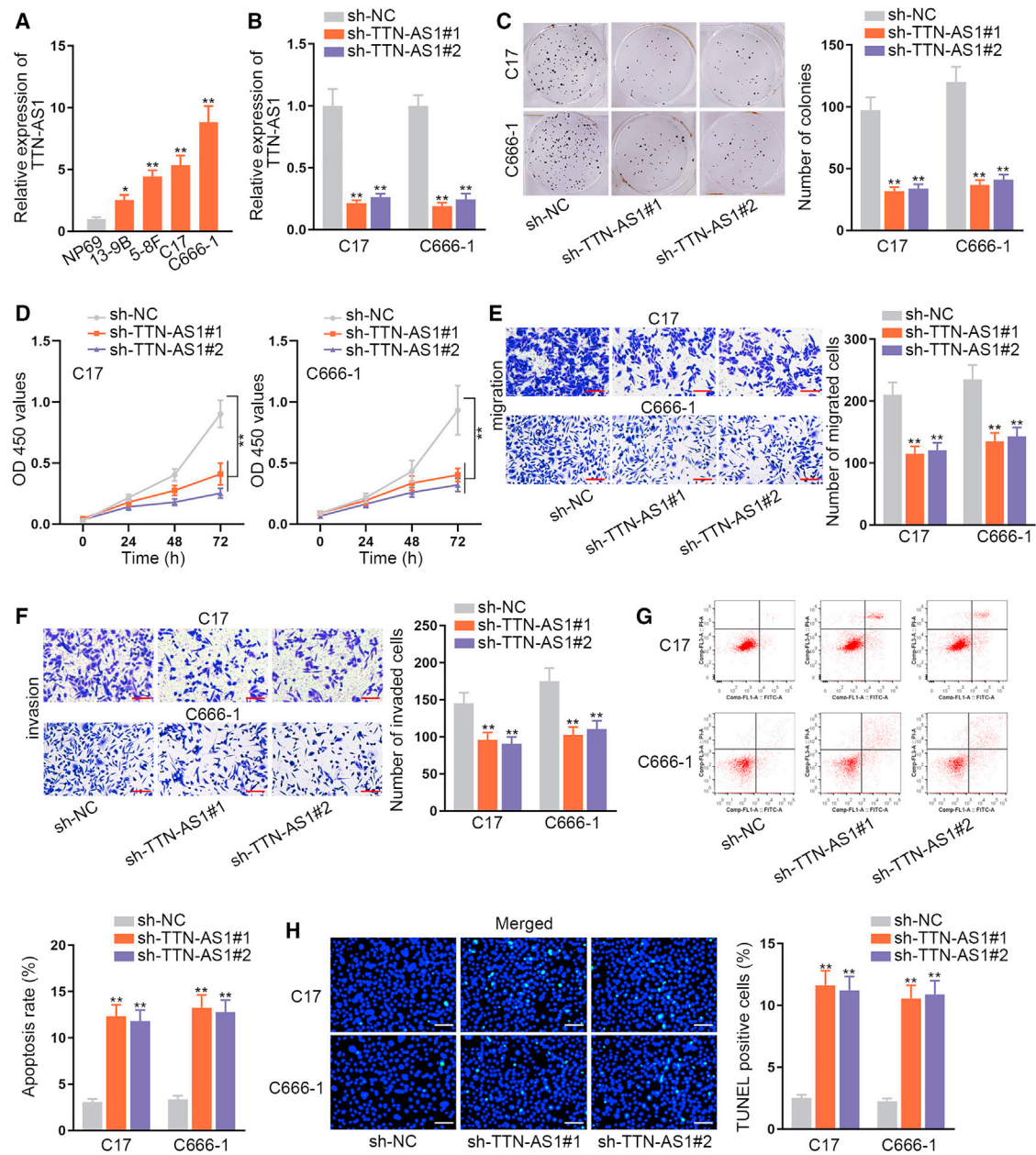


**Figure 1. TTN-AS1 is upregulated in NPC cells relative to NP69 cells and promotes NPC cell growth**

(A) TTN-AS1 expression was detected in NPC cell lines (13-9B, 5-8F, C17, and C666-1) and normal human nasopharyngeal epithelial cells (NP69). (B) The expression of TTN-AS1 in C17 and C666-1 cells transfected with sh-TTN-AS1#1/2 was displayed. (C and D) Proliferation of C17 and C666-1 cells with or without TTN-AS1 deficiency was evaluated. (E and F) Migration and invasion of C17 and C666-1 cells were detected before and after TTN-AS1 knockdown Scale bar = 200µm, Scale bar = 200µm. (G and H) Apoptosis rate of C17 and C666-1 cells was analyzed before and after TTN-AS1 depletion Scale bar = 100µm. Data obtained from three or more than three independent experimental results were shown as mean±SD.\*p < 0.05, \*\*p < 0.01.

we discovered that downregulating NETO2 overtly hampered cell proliferation (Figures 3I and 3J), migration, and invasion (Figures 3K and 3L), while enhancing cell apoptosis (Figures 3M and 3N). In summary, NETO2 is targeted by miR-876-5p and contributes to NPC cell growth.

**TTN-AS1 depends on NETO2 to work as a tumor-facilitator in NPC cells**

The rescue assays were designed to attest the function of the TTN-AS1/NETO2 axis in NPC cells. In the beginning, we overexpressed NETO2 by transfecting pcDNA3.1/NETO2 into NPC cells (Figures

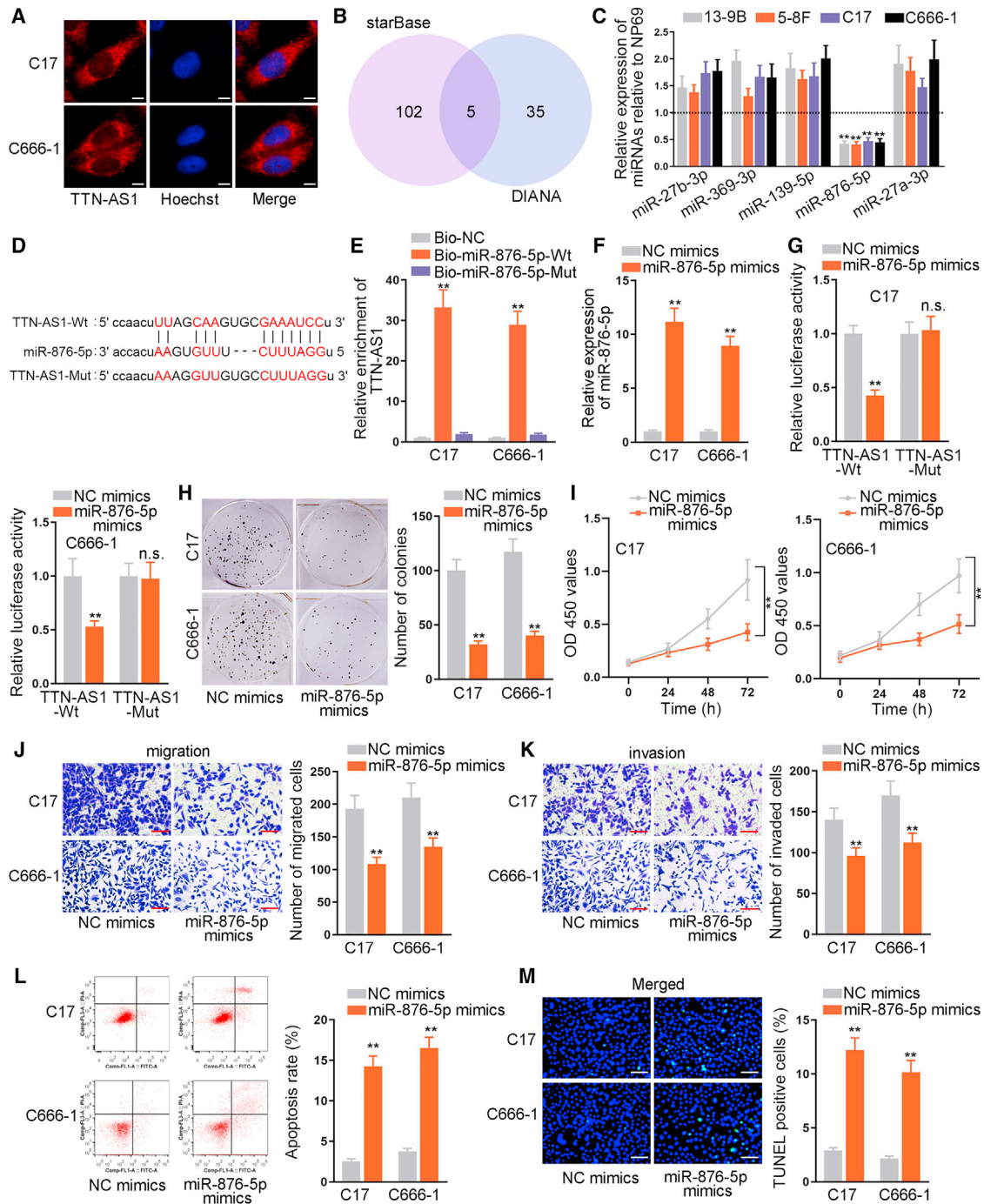


**Figure 2. MiR-876-5p represses the malignant behaviors of NPC cells**

(A) The location of TTN-AS1 in C17 and C666-1 cells was displayed Scale bar = 10 $\mu$ m. (B) StarBase and DIANA were utilized to predict miRNAs which had binding sites with TTN-AS1. (C) Expressions of five miRNAs were tested in NPC cell lines relative to NP69 cells. (D) Bioinformatics tools were applied to predict the binding sites between miR-876-5p and TTN-AS1. (E) The binding affinity between miR-876-5p and TTN-AS1 in C17 and C666-1 cells was assessed. (F) MiR-876-5p expression was quantified in C17 and C666-1 cells with or without transfection of miR-876-5p mimics. (G) Relative luciferase activity was detected to assess the interactive relation between miR-876-5p and TTN-AS1. (H–M) The effects of miR-876-5p on NPC cell proliferation, migration, invasion, and apoptosis were evaluated in NPC cells transfected with miR-876-5p mimics and NC mimics Scale bar = 200 $\mu$ m, Scale bar = 200 $\mu$ m, Scale bar = 100 $\mu$ m. Data obtained from three or more than three independent experimental results were shown as mean $\pm$ SD. \*\* $p$  < 0.01; n.s., not significant.

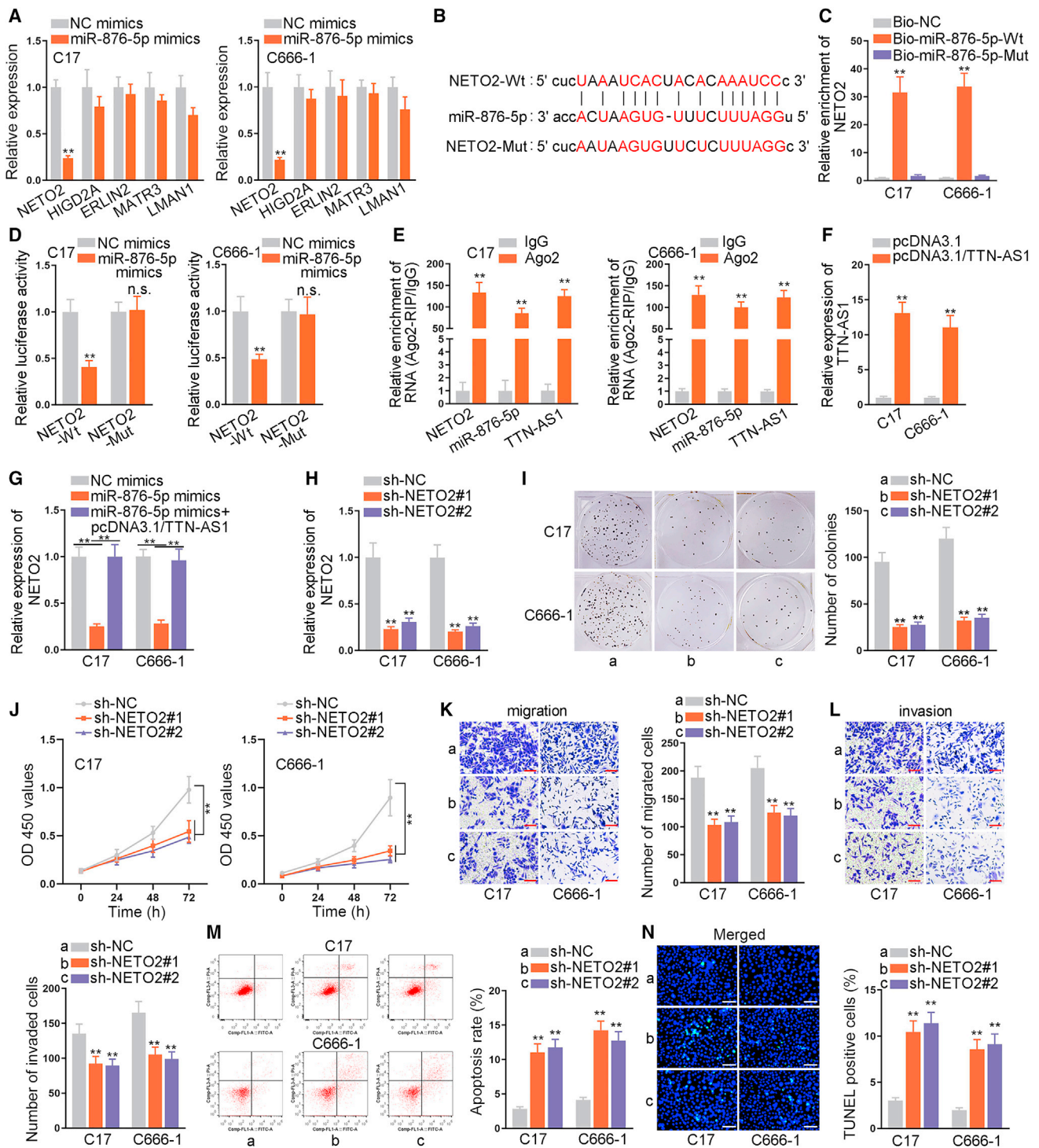


**Figure 3. NETO2 prompts the proliferation, migration and invasion of NPC cells but inhibits cell apoptosis**

(A) The expression of 5 mRNAs was examined in C17 and C666-1 cells with or without miR-876-5p augmentation. (B) Binding sites between miR-876-5p and NETO2 were predicted. (C) The enrichment of NETO2 in Bio-NC, Bio-miR-876-5p-Wt/Mut was quantified. (D) The binding affinity between miR-876-5p and NETO2 was appraised based on the luciferase activity of NETO2-Wt/Mut in C17 and C666-1 cells transfected with miR-876-5p mimics. (E) The enrichment of NETO2, TTN-AS1, and miR-876-5p in RISCs was examined. (F) TTN-AS1 expression was assessed in C17 and C666-1 cells transfected with pcDNA3.1/TTN-AS1. (G) NETO2 expression was detected in C17 and

(legend continued on next page)

4A and S1E). Through conducting colony formation and CCK-8 assays, we noticed that the suppressive cell proliferation caused by TTN-AS1 silencing was recovered after NETO2 upregulation (Figures 4B and 4C). Furthermore, the inhibition on migration and invasion imposed by TTN-AS1 knockdown was offset by augmentation of NETO2 (Figures 4D and 4E). In contrast, the increased apoptosis rate mediated by TTN-AS1 deficiency was reversed by upregulated NETO2 (Figures 4F and 4G). To summarize, TTN-AS1 could improve the proliferative, migratory, and invasive capabilities but inhibit apoptotic ability of NPC cells by regulating NETO2.

#### TTN-AS1 mediates the *in vivo* NPC tumorigenesis via regulating NETO2

Subsequently, we planned to elucidate the influence of TTN-AS1 on NPC tumorigenesis *in vivo*. As manifested in Figure S2A, TTN-AS1 reduction restricted *in vivo* tumor growth, while such inhibition was counteracted upon further elevation of NETO2. Moreover, the volume and weight of excised xenograft tumors were much smaller due to reduced TTN-AS1 levels, while such reduction was counteracted by NETO2 upregulation (Figures S2B and S2C). In sum, TTN-AS1 facilitates NPC tumorigenesis via upregulating NETO2.

#### YY1 accelerates the transcription of TTN-AS1 in NPC cells

After investigating the downstream targets of TTN-AS1, we explored its upstream factors. UCSC (<http://genome.ucsc.edu/>) and JASPAR (<http://jaspar.genereg.net/analysis>) predicted YY1 as the candidate transcription factor of TTN-AS1. Referring to previous literature, YY1 has already been identified to be a transcription activator in multiple cancer-linked researches.<sup>20,21</sup> Hence, we wondered whether YY1 could activate TTN-AS1 in NPC cells. The DNA motif of YY1 was acquired from JASPAR, through which we also found two YY1 binding sites in the TTN-AS1 promoter region (Figure 5A). First, qRT-PCR and western blot assays were performed to detect the expression of YY1 in NP69 and NPC cells. The collected data demonstrated that YY1 expression was higher in NPC cells than NP69 cells (Figure S3A). Moreover, qRT-PCR and western blot results validated the reduced or enhanced expression of YY1 after sh-YY1#1/2 or pcDNA3.1/YY1 was respectively transfected in C17 and C666-1 cells (Figures 5B and S3B). Next, we found TTN-AS1 expression was reduced by YY1 knockdown and augmented by upregulation of YY1 (Figure 5C). Data from chromatin immunoprecipitation (ChIP) assays revealed that YY1 could bind with TTN-AS1 promoter-Wt rather than TTN-AS1 promoter-Mut (Figure 5D). Moreover, data obtained from luciferase reporter assays disclosed that overexpression of YY1 could increase the luciferase activity of TTN-AS1 promoter-Wt remarkably, while such promotion was partly abated when one YY1 binding site in the TTN-AS1 promoter was mutated, and no changes could be

seen when both sites were mutated (Figure 5E). Based on these facts, we deduced that both sites 1 and 2 were effective binding sites of YY1 on TTN-AS1 promoter. To conclude, the transcription factor YY1 facilitates TTN-AS1 transcription in NPC cells.

#### TTN-AS1 recruits UPF1 to enhance NETO2 expression

Various articles have reported that lncRNAs could bind to RBPs to affect the stability of mRNAs.<sup>22-24</sup> Thus, we guessed that some RBPs binding with TTN-AS1 might participate in TTN-AS1-mediated functions in NPC cells. As manifested in Figure 6A, the results of mass spectrometry revealed that certain proteins had strong affinities with TTN-AS1. Previous research has reported that UPF1 can make a difference to cancer progression by stabilization or destabilization of RNA.<sup>25,26</sup> Therefore, we further performed western blot assays. The collected western blots indicated that UPF1 was pulled down by TTN-AS1, rather than by TTN-AS1 antisense, for which we chose UPF1 for the following analysis. Subsequently, the outcomes of RIP assays corroborated that TTN-AS1 was noticeably enriched in anti-UPF1 (Figure 6B). Next, the results of RNA protein pull-down and RIP assays indicated the interaction of NETO2 with UPF1 in NPC cells as well (Figures 6C and 6D). The subsequent RIP assay verified that NETO2 enrichment was decreased in the anti-UPF1 group after knockdown of TTN-AS1 (Figure 6E), which indicated that TTN-AS1 facilitated the interaction of UPF1 with NETO2. In addition, we examined the efficient knockdown of sh-UPF1#1/2 in C17 and C666-1 cells through qRT-PCR and western blot assays (Figure S3C). Taken together, TTN-AS1 recruits UPF1 to stabilize NETO2.

## DISCUSSION

Since the discovery of a large number of ncRNAs, targeted therapy has become a hotspot in the treatment of diseases. Increasing essays explore the function of lncRNAs in cancers. For example, lncRNA PVT1 modulates NPC cell proliferative ability through activating the KAT2A acetyltransferase and enhancing HIF-1 $\alpha$  stability.<sup>27</sup> NKILA restricts NPC carcinogenesis and metastasis via inhibiting the nuclear factor  $\kappa$ B pathway.<sup>28</sup> Moreover, lncRNA H19 boosts NPC proliferation and metastasis in a let-7-dependent manner.<sup>29</sup> Recently, TTN-AS1 has been found to facilitate the progression of gastric cancer via binding with miR-376b-3p.<sup>30</sup> TTN-AS1 enhances the invasive and migratory abilities of lung adenocarcinoma cells by regulating the miR-4677-3p/ZEB1 axis.<sup>31</sup> Also, a former study has corroborated that TTN-AS1 facilitated cell proliferative, migratory, and invasive abilities in prostate cancer.<sup>32</sup> In this study, we confirmed that TTN-AS1 was highly expressed in NPC cells. Next, the loss-of-function assays showed that TTN-AS1 silencing suppressed cell proliferative, migratory, and invasive process but promoted NPC cell apoptosis. We revealed that TTN-AS1 worked as a tumor-facilitator in NPC cells, which was consistent with its

C666-1 cells respectively co-transfected with NC mimics, miR-876-5p mimics, or miR-876-5p mimics + pcDNA3.1/TTN-AS1. (H) NETO2 expression was evaluated in C17 and C666-1 cells with NETO2 knockdown. (I-N) The effects of NETO2 depletion on cell proliferative, migratory, and invasive capabilities as well as the apoptotic ability were examined in C17 and C666-1 cells successfully transfected with sh-NC or sh-NETO2#1/2. Scale bar = 200 $\mu$ m, Scale bar = 200 $\mu$ m, Scale bar = 100 $\mu$ m. Data obtained from three or more than three independent experimental results were shown as mean $\pm$ SD. \*\*p < 0.01; n.s., not significant.

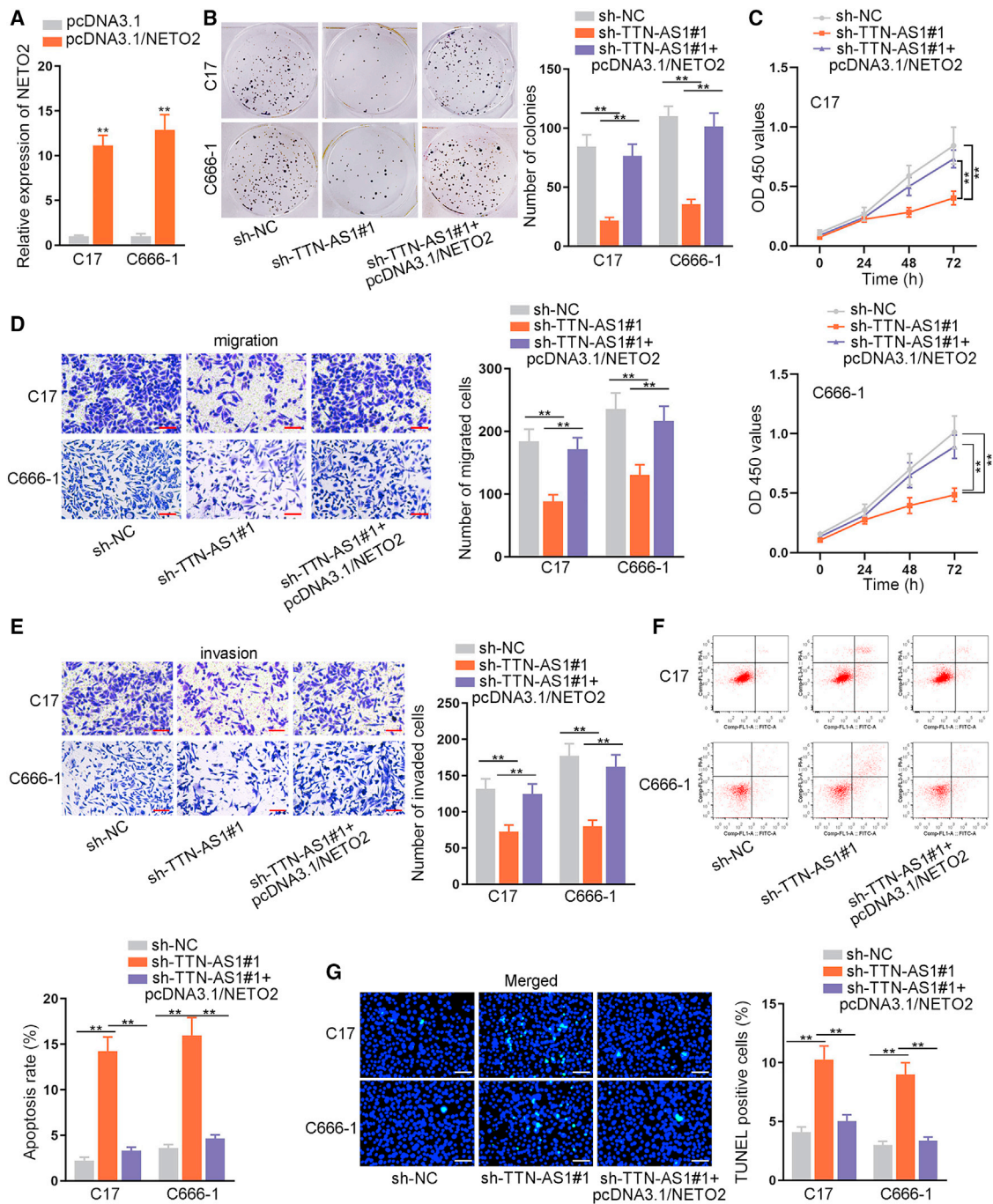


**Figure 4. TTN-AS1 depends on NETO2 to function in NPC cells**

(A) NETO2 expression was assessed in C17 and C666-1 cells after transfection with pcDNA3.1/NETO2. (B–G) The rescue assays were carried out to investigate the proliferation, migration, invasion, and apoptosis of C17 and C666-1 cells in response to different treatments, including sh-NC, sh-TTN-AS1#1, and sh-TTN-AS1#1 + pcDNA3.1/NETO2. Scale bar = 200µm, Scale bar = 200µm, Scale bar = 100µm. Data obtained from three or more than three independent experimental results were shown as mean±SD. \*\*p < 0.01.

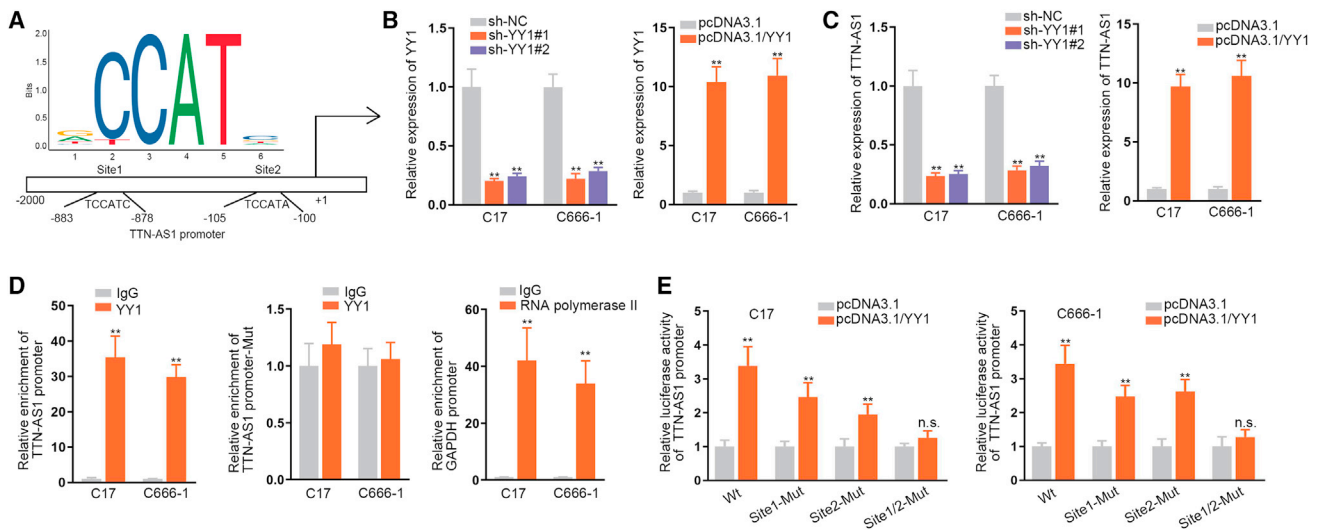


**Figure 5. YY1 accelerates transcription of TTN-AS1 in NPC cells**

(A) Binding sites between TTN-AS1 promoter region and YY1 were presented. (B) The expression of YY1 was detected in C17 and C666-1 cells with YY1 depletion or YY1 augmentation. (C) TTN-AS1 expression was detected after sh-YY1#1/2 and pcDNA3.1/YY1 were transfected into C17 and C666-1 cells. (D) The binding affinity between YY1 protein and TTN-AS1 promoter was assessed. (E) The predicted binding sites of YY1 and TTN-AS1 promoter were examined in C17 and C666-1 cells. \*\* $p < 0.01$ ; n.s., not significant.

function described previously in gastric cancer, lung adenocarcinoma, and prostate cancer.

LncRNAs could work as sponges of miRNAs to exert functions in the ceRNA system. For example, FAM225A contributes to NPC tumorigenesis and metastasis via serving as ceRNA to competitively bind with miR-590-3p/miR-1275 and enhance ITGB3 expression.<sup>33</sup> LncRNA HCG18 boosts NPC progression via the modulation of miR-140/CCND1 and the Hedgehog signaling pathway.<sup>34</sup> TTN-AS1 has been discovered to play an oncogenic role in colorectal cancer by regulating KLF15.<sup>35</sup> In our study, we suggested the ceRNA model of TTN-AS1 by localizing its place in the cytoplasm. Then, miR-876-5p, which was proved to be poorly expressed among NPC cell lines, was selected as the downstream of TTN-AS1 in NPC cell lines. Subsequently, augmentation of miR-876-5p was revealed to repress the malignant behaviors of NPC cells. The former study has validated that miR-876-5p inhibits breast cancer progression via modulating TFAP2A,<sup>36</sup> which was in line with our discovery. Furthermore, we showed that NETO2 was the downstream target of miR-876-5p. A previous study has found that NETO2 boosts cell invasion and migration by targeting the PI3K/AKT/NF-KB/snail axis and could act as a biomarker in gastric cancer.<sup>37</sup> In our study, we discovered that NETO2 had oncogenic functions in NPC cells. In addition, the rescue assays manifested that overexpression of NETO2 could counteract the influence of TTN-AS1 knockdown on NPC cells. Furthermore, *in vivo* assays verified that NETO2 also participated in TTN-AS1-promoted *in vivo* tumorigenesis of NPC. In accordance with the abovementioned literature, we also found that NETO2 played an oncogenic role in NPC. On the whole, TTN-AS1 enhanced

NETO2 expression to facilitate the malignant behaviors of NPC cells via sequestering miR-876-5p.

Moreover, we found that UPF1 could bind to TTN-AS1 in NPC cells. UPF1 has been reported to accelerate the decay of RNA.<sup>38</sup> However, a recent report has also suggested the RNA stabilization role of UPF1 in glioblastoma cells.<sup>26</sup> In this study, we identified UPF1 as the molecular chaperone of TTN-AS1, and that it also interacted with NETO2 mRNA in NPC cells. More importantly, the binding of UPF1 to NETO2 was hindered when TTN-AS1 was silenced in NPC cells. In other words, TTN-AS1 recruited UPF1 to stabilize NETO2 mRNA, so as to upregulate NETO2 expression in NPC cells. As mentioned above, UPF1 has been identified to strengthen the stability of RNA in glioblastoma cells, which was in tune with our findings here.

In conclusion, our study found that YY1-activated TTN-AS1 could expedite the progression of NPC via targeting miR-876-5p/UPF1/NETO2 signaling. Targeting TTN-AS1 could be a potential method to improve the treatment of NPC. Further studies are needed to analyze the appliance of TTN-AS1 in clinic practice in the future.

## MATERIALS AND METHODS

### Cell culture

Human NPC cell lines (13-9B, 5-8F, C17, and C666-1) and normal human nasopharyngeal epithelial cells (NP69) were procured from the American Type Culture Collection (Rockville, MD). All cells were allowed to grow with 10% fetal bovine serum (FBS) and 1% Pen/Strep in DMEM (Invitrogen, Carlsbad, CA) under 37°C and 5% CO<sub>2</sub>.



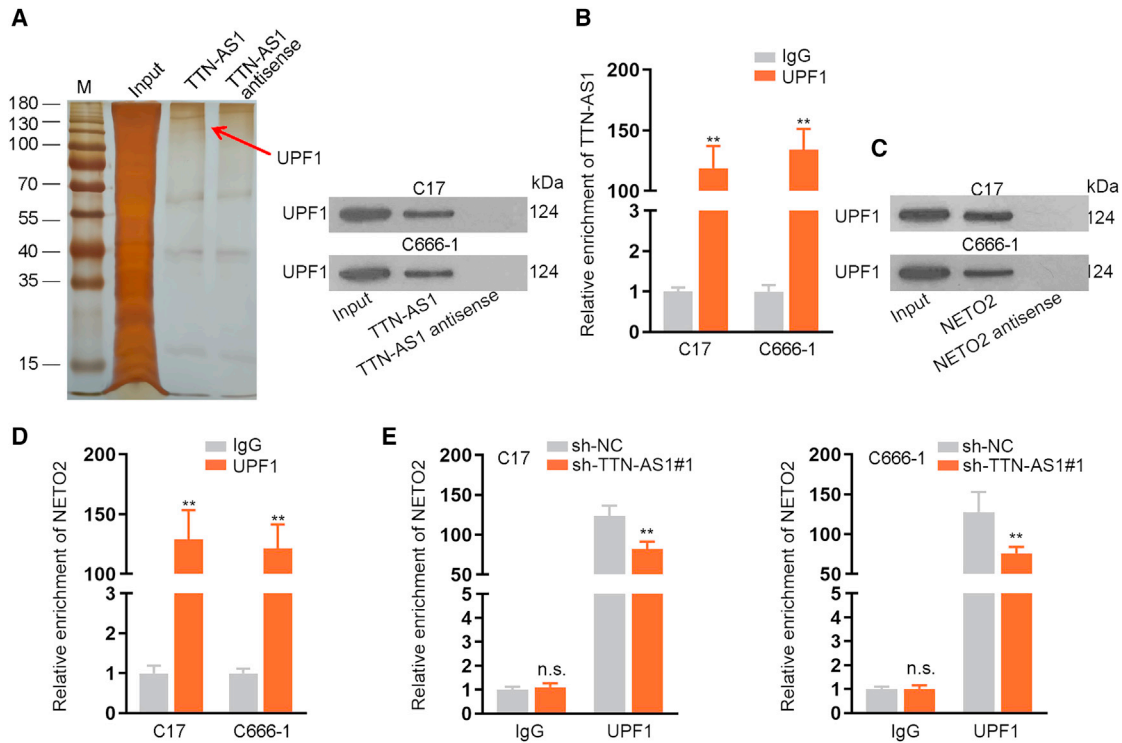


**Figure 6. TTN-AS1 strengthens the binding of UPF1 and NETO2 in NPC cells**

(A) The binding relationship of UPF1 and TTN-AS1 was detected. (B) The interaction of TTN-AS1 and UPF1 was evaluated in C17 and C666-1 cells. (C and D) The affinity between NETO2 and UPF1 in C17 and C666-1 cells was examined. (E) NETO2 precipitated by IgG or UPF1 antibody was quantified in sh-NC and sh-TTN-AS1#1 groups. \*\* $p < 0.01$ ; n.s., not significant.

#### qRT-PCR

Total RNA extraction in cell samples was achieved by TRIzol reagent (Invitrogen). The extracted RNA was then subjected to reverse transcription using the PrimeScript RT reagent kit (TaKaRa, Shiga, Japan) as required. SYBR Premix Ex Taq II (TaKaRa) was applied to evaluate gene expression. The  $2^{-\Delta\Delta Ct}$  method was utilized to calculate the results of qRT-PCR. GAPDH or U6 was defined as the internal reference. The primers were as followed:

5'-GGGAGAAGCTGAGTCATGGG-3' (GAPDH-forward),

5'-TCCCAGTGACATTACAGCC-3' (GAPDH-reverse),

5'-CGCGATATGGTTTTGGCAGG-3' (U6-forward),

5'-TGGACGTATTCGATCAGCCG-3' (U6-reverse),

5'-AGTGGATTTCTTTGTGAA-3' (miR-876-5p-forward),

5'-CTCAACTGGTGTCTGTGGA-3' (miR-876-5p-reverse),

5'-GGTTTTGTGGAGGGCGTAGA-3' (TTN-AS1-forward),

5'-ATGTCAACAGAGGGCGACAG-3' (TTN-AS1-reverse),

5'-ACGGCTTCGAGGATCAGATTC-3' (YY1-forward),

5'-TGACCAGCGTTTGTTCATGT-3' (YY1-reverse),

5'-AGATGGGCCATTTGGTTTCTC-3' (NETO2-forward),

5'-TGCTCGAAATCCCAGTCCTTC-3' (NETO2-reverse).

#### Western blot

Cells were lysed using RIPA buffer (R0278, Sigma-Aldrich, St. Louis, MO, USA). Extracted proteins separated by SDS-PAGE (1610174, Bio-Rad Laboratories, Shanghai, China) were moved to PVDF membrane (IPVH00010, Millipore, Bedford, MA, USA). After membranes were sealed with 5% nonfat milk, primary antibodies including Anti-NETO2 (ab109288, Abcam, Cambridge, MA, UK), Anti-YY1 (ab109228, Abcam), Anti-UPF1 (9435, Cell Signaling Technology, Danvers, MA, USA), and Anti-GAPDH (ab8245, Abcam) were added for incubation overnight at 4°C. GAPDH was used as an internal reference. Later, the membranes were incubated with secondary antibody at room temperature for 1 h. The western blots were finally subject to enhanced chemiluminescence detection.

#### Plasmid transfection

The designed shRNAs (Ribobio, Guangzhou, China) and negative control (sh-NC) for TTN-AS1, NETO2, or YY1 were co-transfected

into C666-1 and C17 cells using Lipofectamine (2000) (Invitrogen). The pcDNA3.1/TTN-AS1, pcDNA3.1/NETO2, pcDNA3.1/YY1, and the empty pcDNA3.1, along with miR-876-5p mimics and NC mimics, were designed by GenePharma (Shanghai, China). Transfected cells were collected after 48 h.

#### Colony formation assay

Clonogenic C666-1 and C17 cells were plated in 6-well plates with 500 cells each well for a 14-day culture. Colonies were then treated with 4% paraformaldehyde for fixation and 0.1% crystal violet for staining. The colonies were then counted manually.

#### CCK-8 assay

Transfected C666-1 and C17 cells were placed on 96-well plates at  $2 \times 10^4$  cells/well, and then cell viability was assessed every 24 h using CCK-8 kit as instructed by the supplier (Dojindo, Kumamoto, Japan). Absorbance at 450 nm was examined by means of microplate reader.

#### Transwell assay

The upper chamber of transwell inserts (Corning, Corning, NY) was added with transfected cell samples in serum-free medium for cell migration assay, and the lower chamber was filled with complete culture medium, which contained 10% FBS. Matrigel (Clontech, Madison, WI) was applied to pre-coat the upper chamber for cell invasion assay. After 24 h of cultivation, cells migrated or invaded to the bottom were fixed with methanol, and treated with 0.1% crystal violet. Finally, cells were observed in five random fields with a light microscope.

#### Flow cytometry analysis

The processed cell samples ( $2 \times 10^5$ ) were collected and rinsed in precooled PBS, and then the cells were stained using an Annexin V-FITC/PI Apoptosis kit (BD Biosciences, San Jose, CA) as instructed. Cells were incubated at room temperature for 15 min, and finally analyzed using a flow cytometer (BD Biosciences).

#### TUNEL assay

C17 and C666-1 cells on coverslips were fixed for 10 min. Then, the samples were rinsed in cold PBS, followed by permeabilization in 0.1% Triton X-100. We used an In Situ Cell Apoptosis Detection Kit (Roche, Basel, Switzerland) for the detection of cell apoptosis. Following the staining of cell nuclei with DAPI dye, cells were observed using a fluorescence microscope (Nikon, Tokyo, Japan).

#### FISH

RNA FISH probes designed for TTN-AS1 were obtained from Ribobio and utilized in line with the user manual. After fixation, the dehydrated cell samples were air dried for hybridization with a TTN-AS1 probe. Samples were then dyed in Hoechst solution, and the staining was finally visualized using a fluorescence microscope.

#### RNA pull-down assay

For the RNA pull-down assay, we used a Pierce Magnetic RNA-Protein Pull-Down Kit (Thermo Fisher Scientific, Waltham, MA). Cell

extracts were mixed with the biotin-labeled probes for miR-876-5p (Bio-NC, Bio-miR-876-5p-Wt, and Bio-miR-876-5p-Mut), TTN-AS1 (sense and antisense), or NETO2 (sense and antisense). After magnetic beads were added, the enriched RNAs and proteins were examined using qRT-PCR or western blot assays as needed.

#### Luciferase reporter assay

TTN-AS1 or NETO2 fragments covering miR-876-5p target sequences (Wt and Mut) were inserted into pmirGLO luciferase vector, termed TTN-AS1-Wt/Mut and NETO2-Wt/Mut. Mutated binding sites were acquired via mutating the nucleotides on TTN-AS1 or NETO2 that were complementary to miR-876-5p. Then the recombinant reporters were co-transfected with miR-876-5p mimics or NC mimics into C666-1 and C17 cells. Moreover, cells in 24-well plates were co-transfected with pGL3-basic vector covering the TTN-AS1 promoter and pcDNA3.1/YY1 or empty pcDNA3.1. The luciferase activity was finally measured using a Luciferase Reporter Assay System (Promega, Fitchburg, WI).

#### RIP

Tumor cells were first lysed in RIP lysis buffer, and the collected cell lysates were conjugated with human anti-Ago2 antibody or UPF1 antibody in magnetic beads. Normal mouse IgG antibody was applied for the control groups. All antibodies were acquired from Millipore (Billerica, MA). The precipitates were examined using qRT-PCR.

#### ChIP

ChIP assay was implemented in C666-1 and C17 cells in line with the user guidebook for the EZ-ChIP Kit (Millipore). The crosslinked chromatin was prepared, sonicated, and then immunoprecipitated with anti-YY1, anti-RNA polymerase II, or anti-IgG antibody conjugated with magnetic beads. qPCR was carried out to detect the enrichment of DNA fragments in ChIP products. An RNA polymerase II-GAPDH promoter group served as positive control in this assay.

#### Tumor xenograft model

BALB/c nude mice (4- to 5-week-old, 18–20 g) were obtained from Shanghai SLAC Laboratory Animal Co. Ltd. (Shanghai, China). C17 cells ( $1 \times 10^6$  per injection) that were respectively transfected with sh-NC, sh-TTN-AS1#1, or sh-TTN-AS1#1 + pcDNA3.1/NETO2 were inoculated into the right flank of mice via subcutaneous injection. Tumor growth was monitored every 4 days and a caliper was utilized to measure tumor size. Tumor size was calculated after tumors could be apparently observed based on the following formula: volume = (length  $\times$  width<sup>2</sup>)/2. Tumor weights were measured using electronic scales. After 4 weeks, all mice were sacrificed via cervical dislocation. The animal experiments were approved by the Animal Care and Use Committee of Hainan Hospital affiliated to Hainan Medical College.

#### Statistical analyses

All experiments were bio-repeated individually in triplicate. Results were presented as mean  $\pm$  standard deviation (SD) after being

processed by PRISM 6 (GraphPad, San Diego, CA). The threshold of statistical significance was set as *p* value below 0.05, which was analyzed by Student's *t* test, one-way analysis of variance (ANOVA), or two-way ANOVA.

## SUPPLEMENTAL INFORMATION

Supplemental information can be found online at <https://doi.org/10.1016/j.omto.2021.11.009>.

## ACKNOWLEDGMENTS

We sincerely appreciate all lab members. This work was supported by the National Natural Science Foundation of China (81960389) and the Academician Innovation Platform of Hainan Province.

## AUTHOR CONTRIBUTIONS

X.C. led this study and designed the experiments. Z.M., J.Z., J.H., and W.X. performed the experiments and analyzed the data. X.L. prepared the figures. S.F. wrote the manuscript. All authors read and approved the final manuscript.

## DECLARATION OF INTERESTS

The authors declare no competing interests.

## REFERENCES

- Kong, L., Li, X., Wang, H., He, G., and Tang, A. (2018). Calycosin inhibits nasopharyngeal carcinoma cells by influencing EWSAT1 expression to regulate the TRAF6-related pathways. *Biomed. Pharmacother.* *106*, 342–348.
- Lin, C., Zong, J., Lin, W., Wang, M., Xu, Y., Zhou, R., Lin, S., Guo, Q., Chen, H., Ye, Y., et al. (2018). EBV-miR-BART8-3p induces epithelial-mesenchymal transition and promotes metastasis of nasopharyngeal carcinoma cells through activating NF-kappaB and Erk1/2 pathways. *J. Exp. Clin. Cancer Res.* *37*, 283.
- Lyu, X., Wang, J., Guo, X., Wu, G., Jiao, Y., Faleti, O.D., Liu, P., Liu, T., Long, Y., Chong, T., et al. (2018). EBV-miR-BART1-5P activates AMPK/mTOR/HIF1 pathway via a PTEN independent manner to promote glycolysis and angiogenesis in nasopharyngeal carcinoma. *PLoS Pathog.* *14*, e1007484.
- Chao, H.L., Liu, S.C., Tsao, C.C., Lin, K.T., Lee, S.P., Lo, C.H., Huang, W.Y., Liu, M.Y., Jen, Y.M., and Lin, C.S. (2017). Dose escalation via brachytherapy boost for nasopharyngeal carcinoma in the era of intensity-modulated radiation therapy and combined chemotherapy. *J. Radiat. Res.* *58*, 654–660.
- Yan, H., Cao, X., and Wang, J. (2017). Application of intensity-modulated radiation therapy in the treatment of nasopharyngeal carcinoma. *Oncol. Lett.* *14*, 7773–7776.
- Zhang, L., Huang, Y., Hong, S., Yang, Y., Yu, G., Jia, J., Peng, P., Wu, X., Lin, Q., Xi, X., et al. (2016). Gemcitabine plus cisplatin versus fluorouracil plus cisplatin in recurrent or metastatic nasopharyngeal carcinoma: a multicentre, randomised, open-label, phase 3 trial. *Lancet.* *388*, 1883–1892.
- Bhan, A., Soleimani, M., and Mandal, S.S. (2017). Long noncoding RNA and cancer: a new paradigm. *Cancer Res.* *77*, 3965–3981.
- Wen, X., Liu, X., Mao, Y.P., Yang, X.J., Wang, Y.Q., Zhang, P.P., Lei, Y., Hong, X.H., He, Q.M., Ma, J., et al. (2018). Long non-coding RNA DANCR stabilizes HIF-1alpha and promotes metastasis by interacting with NF90/NF45 complex in nasopharyngeal carcinoma. *Theranostics* *8*, 5676–5689.
- Hu, W., Xu, W., Shi, Y., and Dai, W. (2018). lncRNA HOTAIR upregulates COX-2 expression to promote invasion and migration of nasopharyngeal carcinoma by interacting with miR-101. *Biochem. Biophys. Res. Commun.* *505*, 1090–1096.
- Lian, Y., Xiong, F., Yang, L., Bo, H., Gong, Z., Wang, Y., Wei, F., Tang, Y., Li, X., Liao, Q., et al. (2018). Long noncoding RNA AFAP1-AS1 acts as a competing endogenous RNA of miR-423-5p to facilitate nasopharyngeal carcinoma metastasis through regulating the Rho/Rac pathway. *J. Exp. Clin. Cancer Res.* *37*, 253.
- Chen, P., Wang, R., Yue, Q., and Hao, M. (2018). Long non-coding RNA TTN-AS1 promotes cell growth and metastasis in cervical cancer via miR-573/E2F3 503, 2956–2962.
- Fu, D., Lu, C., Qu, X., Li, P., Chen, K., Shan, L., and Zhu, X. (2019). lncRNA TTN-AS1 regulates osteosarcoma cell apoptosis and drug resistance via the miR-134-5p/MBTD1 axis. *Biochem. Biophys. Res. Commun.* *11*, 8374–8385.
- Liang, J., Li, H., Han, J., Jiang, J., Wang, J., Li, Y., Feng, Z., Zhao, R., Sun, Z., Lv, B., et al. (2020). Mex3a interacts with LAMA2 to promote lung adenocarcinoma metastasis via PI3K/AKT pathway. *Cell Death Dis.* *11*, 614.
- Lin, C., Zhang, S., Wang, Y., Wang, Y., Nice, E., Guo, C., Zhang, E., Yu, L., Li, M., Liu, C., et al. (2018). Functional role of a novel long noncoding RNA TTN-AS1 in esophageal squamous cell carcinoma progression and metastasis. *Clin. Cancer Res.* *24*, 486–498.
- Song, Y.X., Sun, J.X., Zhao, J.H., Yang, Y.C., Shi, J.X., Wu, Z.H., Chen, X.W., Gao, P., Miao, Z.F., and Wang, Z.N. (2017). Non-coding RNAs participate in the regulatory network of CLDN4 via ceRNA mediated miRNA evasion. *Nat. Commun.* *8*, 289.
- Li, Z., Hong, S., and Liu, Z. (2018). lncRNA LINC00641 predicts prognosis and inhibits bladder cancer progression through miR-197-3p/KLF10/PTEN/PI3K/AKT cascade. *Biochem. Biophys. Res. Commun.* *503*, 1825–1829.
- Shao, Y., Ye, M., Li, Q., Sun, W., Ye, G., Zhang, X., Yang, Y., Xiao, B., and Guo, J. (2016). lncRNA-RMRP promotes carcinogenesis by acting as a miR-206 sponge and is used as a novel biomarker for gastric cancer. *Oncotarget.* *7*, 37812–37824.
- Ozer, A., Tome, J.M., Friedman, R.C., Gheba, D., Schroth, G.P., and Lis, J.T. (2015). Quantitative assessment of RNA-protein interactions with high-throughput sequencing-RNA affinity profiling. *Nat. Protoc.* *10*, 1212–1233.
- Li, J., Cheng, D., Zhu, M., Yu, H., Pan, Z., Liu, L., Geng, Q., Pan, H., Yan, M., and Yao, M. (2019). OTUB2 stabilizes U2AF2 to promote the Warburg effect and tumorigenesis via the AKT/mTOR signaling pathway in non-small cell lung cancer. *Theranostics* *9*, 179–195.
- Qiao, K., Ning, S., Wan, L., Wu, H., Wang, Q., Zhang, X., Xu, S., and Pang, D. (2019). LINC00673 is activated by YY1 and promotes the proliferation of breast cancer cells via the miR-515-5p/MARK4/Hippo signaling pathway. *J. Exp. Clin. Res.* *38*, 418.
- Hu, Z., Tie, Y., Lv, G., Zhu, J., Fu, H., and Zheng, X. (2018). Transcriptional activation of miR-320a by ATF2, ELK1 and YY1 induces cancer cell apoptosis under ionizing radiation conditions. *Int. J. Oncol.* *53*, 1691–1702.
- Modic, M., Grosch, M., Rot, G., Schirge, S., Lepko, T., Yamazaki, T., Lee, F.C.Y., Rusha, E., Shaposhnikov, D., Palo, M., et al. (2019). Cross-regulation between TDP-43 and paraspeckles promotes pluripotency-differentiation transition. *Mol. Cell* *74*, 951–965.e13.
- Zhang, J., Li, S., Zhang, L., Xu, J., Song, M., Shao, T., Huang, Z., and Li, Y. (2020). RBP EIF2S2 promotes tumorigenesis and progression by regulating MYC-mediated inhibition via FHIT-related enhancers. *Mol. Therapy* *28*, 1105–1118.
- Xu, H., Jiang, Y., Xu, X., Su, X., Liu, Y., Ma, Y., Zhao, Y., Shen, Z., Huang, B., and Cao, X. (2019). Inducible degradation of lncRNA Sros1 promotes IFN- $\gamma$ -mediated activation of innate immune responses by stabilizing Stat1 mRNA. *Nat. Immunol.* *20*, 1621–1630.
- Xie, X., Lin, J., Liu, J., Huang, M., Zhong, Y., Liang, B., Song, X., Gu, S., Chang, X., Huang, D., et al. (2019). A novel lncRNA NR4A1AS up-regulates orphan nuclear receptor NR4A1 expression by blocking UPF1-mediated mRNA destabilization in colorectal cancer. *Clin. Sci.* *133*, 1457–1473.
- Shao, L., He, Q., Liu, Y., Liu, X., Zheng, J., Ma, J., Liu, L., Li, H., Li, Z., and Xue, Y. (2019). UPF1 regulates the malignant biological behaviors of glioblastoma cells via enhancing the stability of linc-00313 10, 629.
- Wang, Y., Chen, W., Lian, J., Zhang, H., Yu, B., Zhang, M., Wei, F., Wu, J., Jiang, J., Jia, Y., et al. (2020). The lncRNA PVT1 regulates nasopharyngeal carcinoma cell proliferation via activating the KAT2A acetyltransferase and stabilizing HIF-1 $\alpha$ . *Cell Death Dis.* *27*, 695–710.
- Zhang, W., Guo, Q., Liu, G., Zheng, F., Chen, J., Huang, D., Ding, L., Yang, X., Song, E., Xiang, Y., et al. (2019). NKILA represses nasopharyngeal carcinoma carcinogenesis and metastasis by NF- $\kappa$ B pathway inhibition. *PLoS Genet.* *15*, e1008325.

29. Zhang, Y., Zhu, R., Wang, J., Cui, Z., Wang, Y., and Zhao, Y. (2019). Upregulation of lncRNA H19 promotes nasopharyngeal carcinoma proliferation and metastasis in let-7 dependent manner. *Artif. Cells Nanomed. Biotechnol.* *47*, 3854–3861.
30. Dong, M.M., Peng, S.J., Yuan, Y.N., and Luo, H.P. (2019). LncRNA TTN-AS1 contributes to gastric cancer progression by acting as a competing endogenous RNA of miR-376b-3p. *Neoplasma.* *66*, 564–575.
31. Zhong, Y., Wang, J., Lv, W., Xu, J., Mei, S., and Shan, A. (2019). LncRNA TTN-AS1 drives invasion and migration of lung adenocarcinoma cells via modulation of miR-4677-3p/ZEB1 axis. *J. Cell Biochem.* *120*, 17131–17141.
32. Zhu, Y., Yang, Z., Luo, X.H., and Xu, P. (2019). Long noncoding RNA TTN-AS1 promotes the proliferation and migration of prostate cancer by inhibiting miR-1271 level. *Cell Death Dis.* *10*, 10678–10684.
33. Zheng, Z.Q., Li, Z.X., Zhou, G.Q., Lin, L., Zhang, L.L., Lv, J.W., Huang, X.D., Liu, R.Q., Chen, F., He, X.J., et al. (2019). Long noncoding RNA FAM225A promotes nasopharyngeal carcinoma tumorigenesis and metastasis by acting as ceRNA to sponge miR-590-3p/miR-1275 and upregulate ITGB3. *Eur. Rev. Med. Pharmacol. Sci.* *79*, 4612–4626.
34. Bundgaard, H., and Larsen, J.D. (1988). N-sulfonyl imidates as a novel prodrug form for an ester function or a sulfonamide group. *J. Med. Chem.* *31*, 2066–2069.
35. Wang, Y., Jiang, F., Xiong, Y., Cheng, X., Qiu, Z., and Song, R. (2019). LncRNA TTN-AS1 sponges miR-376a-3p to promote colorectal cancer progression via upregulating KLF15. *Life Sci.* *116*, 936.
36. Xu, J., Zheng, J., Wang, J., and Shao, J. (2019). miR-876-5p suppresses breast cancer progression through targeting TFAP2A. *Exp. Ther. Med.* *18*, 1458–1464.
37. Liu, J.Y., Jiang, L., He, T., Liu, J.J., Fan, J.Y., Xu, X.H., Tang, B., Shi, Y., Zhao, Y.L., Qian, F., et al. (2019). NETO2 promotes invasion and metastasis of gastric cancer cells via activation of PI3K/Akt/NF-kappaB/Snail axis and predicts outcome of the patients. *Cell Death Dis.* *10*, 162.
38. Plank, T.D.M., and Wilkinson, M.F. (2018). RNA decay factor UPF1 promotes protein decay: a hidden talent. *Bioessays* *40*. <https://doi.org/10.1002/bies.201700170>.